Published in final edited form as:
Nat Neurosci. 1999 December ; 2(12): 1131–1136. doi:10.1038/16056.

Dual streams of auditory afferents target multiple domains in the primate prefrontal cortex

L. M. Romanski[1], **B. Tian**[2], **J. Fritz**[3], **M. Mishkin**[3], **P. S. Goldman-Rakic**[1], and **J. P. Rauschecker**[2]

[1] Section of Neurobiology, B-413 SHM, 333 Cedar St., Yale University School of Medicine, New Haven, Connecticut, USA

[2] Georgetown Institute for Cognitive and Computational Science, Georgetown University Medical Center, New Research Bldg., Rm. WP15, 3970 Reservoir Road NW, Washington, DC 20007-2197, USA

[3] Laboratory of Neuropsychology, National Institute of Mental Health, Building 49, Room 1B80, Bethesda, Maryland 20892-4415, USA

Abstract

'What' and 'where' visual streams define ventrolateral object and dorsolateral spatial processing domains in the prefrontal cortex of nonhuman primates. We looked for similar streams for auditory–prefrontal connections in rhesus macaques by combining microelectrode recording with anatomical tract-tracing. Injection of multiple tracers into physiologically mapped regions AL, ML and CL of the auditory belt cortex revealed that anterior belt cortex was reciprocally connected with the frontal pole (area 10), rostral principal sulcus (area 46) and ventral prefrontal regions (areas 12 and 45), whereas the caudal belt was mainly connected with the caudal principal sulcus (area 46) and frontal eye fields (area 8a). Thus separate auditory streams originate in caudal and rostral auditory cortex and target spatial and non-spatial domains of the frontal lobe, respectively.

Anatomical, physiological and neuropsychological evidence suggests that visual information is transmitted as distinct 'what' and 'where' processing streams that ultimately terminate within the frontal lobes[1–3]. In contrast, attempts to understand higher auditory processing have not yielded as complete a picture as that of the visual system. Frontal as well as temporal lobe regions have been associated with language processing since the discoveries of Broca and Wernicke. Localization of language function to frontal regions has been confirmed and extended by fMRI and PET imaging during the performance of a wide range of auditory and language tasks including auditory working memory, verbal recall, phonological processing, comprehension and semantic judgement[4–7]. Although anatomical connections exist between the superior temporal gyrus and frontal lobes[8–14], functional characterization of the auditory pathways terminating within the pre-frontal cortex, including those involved in speech and language processing, remains incomplete.

The primate cortical auditory system in the temporal lobe has a concentric organizaton[15]. The central core region, including primary auditory cortex, is located on the supratemporal plane and is encircled by secondary auditory cortices, the belt areas, which are bordered laterally by a parabelt region[16–21] (Fig. 1a and **b**). The lateral belt areas can be distinguished from primary auditory cortex by the presence of neurons with increased responsiveness to complex acoustic stimuli, including band-passed noise and species-specific vocalizations[17], as opposed to to pure

Correspondence should be addressed to L.M.R. (lizabeth.romanski@yale.edu).

tones. Indeed, three cochleotopically organized fields separated by frequency reversals, termed anterolateral (AL), middle-lateral (ML) and caudolateral (CL) areas, are mapped within the lateral belt[17]. Electrophysiological studies of the superior temporal region in nonhuman primates suggests that its anterior and posterior aspects may differ functionally[22,23]. Furthermore, differences also exist between anterior and posterior belt/parabelt connectivity with nearby cortical and thalamic targets[18–21,24]. These findings raise the possibility that separate thalamocortical and corticocortical streams exist in the auditory system just as they do in the visual system[14,18,25].

We combined electrophysiological recording and anatomical tract tracing in Old World monkeys (*Macaca mulatta)* to characterize more precisely the pathways by which acoustic information emanating from defined fields of the auditory association cortex may reach higher cognitive processing areas of the frontal lobes. We provide evidence that separate cochleotopic fields in non-primary auditory cortex are connected with distinct spatial and non-spatial domains of the prefrontal cortex in pathways analogous to visual cortical streams.

Results

We recorded from the lateral auditory belt and parabelt cortices in the superior temporal region of four rhesus macaques and determined the best center frequency along each electrode penetration through lateral belt areas AL, ML and CL. The presence of frequency reversals along the anterior–posterior extent of the superior temporal gyrus identified the cochleotopic boundaries of these fields (Fig. 1). The most anterior field, AL, had neuronal responses that ranged from 12.5 kHz at its most anterior edge down to 0.5 kHz where a frequency reversal occurred at its caudal edge, the point where area ML began. The best center frequencies in ML ranged from 0.5 kHz at its rostral edge to 20 kHz caudally just before the frequency reversal that marked the beginning of the caudal field, CL. The best frequencies in CL ranged from 20 kHz to 1 kHz. At the conclusion of the electrophysiological recordings, four to six distinguishable anatomical tracers were distributed among AL, ML and CL. For two of four cases (Fig. 1e and **f**), a different tracer was injected into the identical frequency region of all three fields, allowing us to determine the possible interactions of region and frequency within the prefrontal cortex. The tracers included both anterograde and retrograde tracers that permitted visualization of whole axonal arbors as they entered different laminae in cortical targets.

In all four experiments, five specific regions of the frontal lobes had labeled retrograde cells and anterograde fibers. These frontal lobe targets included the frontal pole (Fig. 2a), the principal sulcus, the lateral inferior convexity (Fig. 2b and **c**), the lateral orbital cortex (Fig. 2b and **d**) and the dorsal periarcuate region. Moreover, these connections were topographically organized such that projections from AL typically involved the frontal pole (area 10), the rostral principal sulcus (area 46), the inferior convexity (areas 12 vl and 45) and the lateral orbital cortex (areas 11, 12o; Fig. 3a, b and e). In contrast, projections from area CL targeted the dorsal periarcuate cortex (area 8a, frontal eye fields) and the caudal principal sulcus (area 46) as well as the caudal inferior convexity (areas 12 vl and 45; Fig. 3b, c and e) and, in two cases, premotor cortex (area 6d). The frontal pole (area 10) and the lateral orbital cortices (areas 11 and 12) were devoid of anterograde labeling from injections into the caudal auditory region (Fig. 3a, **b** and **e**). Conversely, the frontal eye fields did not receive projections from anterior auditory area AL (Fig. 3c and **e**). Examination of the anterograde and retrograde labeling in the principal sulcus (areas 46) and the inferior convexity (areas 12 and 45), where AL and CL projections converged, revealed a rostrocaudal topography within these convergence zones such that rostral labeling in the principal sulcus and inferior convexity resulted from AL injections (Fig. 3a, **b** and **e**), whereas projections from area CL accounted for caudal labeling in these areas (Fig. 3b, **c** and **e**). ML projections were usually a combination of those from anterior and

posterior fields and involved less of the extreme frontal pole and frontal eye fields but did label the principal sulcus, lateral inferior convexity and lateral orbital cortex (Fig. 3). These highly specific rostrocaudal topographical frontal–temporal connections suggest separate streams of auditory information that target distinct domains of the frontal lobes.

In all regions examined, anterograde and retrograde labeling were regionally co-extensive, although the laminar patterns of labeled cells and axons differed. Retrogradely labeled cells were most commonly observed in layers 3, 5 and 6, whereas anterograde fibers were most commonly found either as patches in layers 1, 5 and 6 or as columns spanning all layers. These observations agree with reports of temporal–prefrontal connections[10–12] and general corticocortical feed-forward and feedback connections[26].

In addition to the frontal lobe targets, the lateral belt regions also projected in a topographic manner to nearby anterior temporal lobe regions and posterior parietal regions, consistent with previous findings[16,18–20]. Projections from areas AL and ML were densest within the rostral parabelt and rostral temporal lobe, including the rostral supratemporal plane. In contrast, the posterior parietal cortex areas 7a and 7ip were labeled from injections only in CL. In addition, the medial belt regions and the caudal half of the dorsal bank of the superior temporal sulcus received dense projections from areas ML and CL but only light projections from AL.

Discussion

Combining electrophysiological recording and anatomical tracing, we demonstrated two pathways originating in separate, non-primary, cochleotopic auditory fields of the superior temporal region and terminating in distinct regions of the frontal lobes (Fig. 3d). One pathway, originating in CL, targets caudal dorsolateral prefrontal cortex (DLPFC); the other pathway, originating in AL, targets rostral and ventral prefrontal areas. Because these dorsal and ventral prefrontal regions are respectively characterized as spatial and non-spatial functional domains[2,27–29], a possible interpretation is that these separate streams originating from posterior and anterior auditory belt and parabelt cortices are analogous to the ‘where’ and ‘what’ streams of the visual system. Although topographic connections between the auditory belt and parabelt cortex and the prefrontal cortex are demonstrated[13,14], these purely anatomical studies are less compelling than the present study in that, without physiology, they could not identify the separate origins of possible auditory streams. We combined the physiological identification of separate auditory cortical fields with multiple injections of anterograde and retrograde anatomical tracers in a nonhuman primate.

The DLPFC is essential in visuospatial working memory, as demonstrated by electrophysiological recording and lesions in primates[27–29] and by imaging in humans[30,31]. Here we showed that the DLPFC also receives auditory afferents from the caudal auditory belt region, suggesting its involvement in auditory processing as well. This is supported by previous studies in nonhuman primates demonstrating that neurons in DLPFC respond to acoustic stimuli and that lesions of the periarcuate and dorsolateral cortex impair auditory conditional responses[32–35]. Specifically, electrophysiological recordings show that the responsiveness of acoustic neurons in the DLPFC depends on sound-source location[33] and that auditory neurons in the periarcuate region are more active during auditory localization than during passive listening[34]. Furthermore, neuroimaging studies demonstrate involvement of the DLPFC in sound localization in humans[36].

Evidence suggests that neurons in the caudal superior temporal region are sensitive to sound-source location[22,23,25] in the same way as their target region, the DLPFC. Neurons in CL and AL have been directly compared for their sensitivity to sound location and for their selectivity for monkey vocalizations (J.P.R., A. Durham, A. Kustov, A. Lord & B. T., *Soc. Neurosci.*

Abstr. **25**, 157.2, 1999). Neurons in AL of anesthetized monkeys presented with acoustic stimuli (consisting of vocalizations and band-passed noise from a variety of different azimuth locations in free field) show better selectivity for particular monkey calls, whereas neurons in CL had significantly narrower spatial tuning. These results confirm previous studies[22,23] and support the notion of an auditory spatial stream originating in the caudal belt and parabelt region and targeting the DLPFC. The caudal belt and parabelt are also connected to the DLPFC via the posterior parietal cortex, which is itself involved in the localization of both visual and auditory signals[36–39].

In addition to this dorsal (and potentially 'spatial') auditory pathway, we present evidence for a second auditory stream originating in the anterior belt and parabelt region and terminating in the rostral and ventral frontal lobe. Neuroimaging studies demonstrate involvement of the frontal pole (area 10) of the rostral frontal lobe in verb generation, auditory working memory and musical consonance[4,7,40].

Neuropsychological research and imaging studies firmly establish involvement of the ventral frontal lobe, including Broca's area and the inferior frontal gyrus, in non-spatial, higher auditory and language processing[4–7,41]. Our results substantiate findings of a connection between the ventral prefrontal cortex and anterior auditory cortical regions[10,14,42]. Ventrolateral frontal lobe regions 12 and 45, which make up the inferior convexity in the nonhuman primate, are situated just anterior to area 6, the premotor cortex[43]; it is suggested, on the basis of anatomical location and connections, that they represent the macaque homolog of Broca's area[42]. Disruption of auditory discrimination performance by lesions of the ventrolateral prefrontal cortex that include the prefrontal inferior convexity or ventral arcuate region[44–46] implies a link between the nonhuman primate ventral frontal lobe and higher auditory processing. Electrophysiological studies also provide some evidence of auditory-responsive neurons in the ventrolateral prefrontal cortex[47–49]. Prefrontal auditory neurons are generally observed as sparsely distributed over a widespread region of the lateral frontal lobe, although in one study, responses of anesthetized monkeys to simple auditory and visual stimuli were localized to the lateral orbital cortex[49]. In contrast, there is substantial evidence of a visual object domain physiologically localized to the inferior convexity region, which has neurons that robustly respond to pictures of objects, patterns and faces[2,50]. Visual physiology together with earlier lesion studies and our present anatomical evidence suggest that the ventrolateral prefrontal cortex may also be devoted to auditory 'pattern' or 'object' processing in the nonhuman primate. Further physiological analysis of ventral prefrontal cortex is needed to examine this possibility.

Our findings also relate to general theories of frontal lobe organization. The observation that both auditory and visual modalities are represented in similar regions of the frontal lobe supports the functional domain hypothesis, which stresses that the frontal lobe is organized into separate dorsolateral spatial-and ventrolateral object-processing regions[27,29]. These domains, specified by distinct afferent inputs, including those presented here, are functionally distinct but extend across modalities.

Methods

Surgery and electrophysiological recordings

Four rhesus macaques (*Macaca mulatta*) were used. All methods were in accordance with NIH *Guidelines for the Care and Use of Laboratory Animals*. Surgical and recording methods were as described previously[17,19]. Electrophysiological recordings were made in macaques anesthetized with isoflurane (1–2%) in a nitrous oxide/oxygen mixture (50:50). The bone overlying the superior temporal gyrus was removed under aseptic surgical conditions and lacquer-insulated tungsten microelectrodes were placed into the belt cortex of the superior

temporal region. Auditory stimuli, including pure tones and band-passed noise (BPN) bursts, were produced using the program SIGNAL (Engineering Design, Belmont, Massachusetts) and presented to the anesthetized monkey. The auditory stimuli were delivered through a power amplifier to a single loudspeaker (Infinity Kappa 5) placed 1.14 m. in front of the monkey. The sound pressure level of the stimuli (measured with a Bruel & Kjaer half-inch condenser microphone and a B & K precision sound level meter) measured at the monkey's head, varied between 60 and 85 dB SPL. The position of each electrode track was digitally acquired (NIH Image) and aligned using blood vessels as reference landmarks (Fig. 1c). Neuronal spike activity was collected, stored and analyzed on a personal computer (Pentium, IBM-compatible). Raster displays and peristimulus time histograms were generated and evaluated in response to the various auditory stimuli. Stimuli were repeated 10–20 times in blocks of 7 different stimuli. An average of 14 electrode tracks per monkey were distributed across the lateral belt cortex of the superior temporal region. At least three responses from single and multiple units were sampled along each electrode track along a depth of approximately 2 mm. A best center frequency (BF_c) was calculated for each penetration by averaging the responses to pure tone and BPN stimuli. Maps of the BF_c for each experiment are shown in Fig. 1.

Injections of both anterograde and retrograde anatomical tracers were made in each of the four monkeys at the end of the electrophysiological recordings. One or two different tracers were placed into AL, ML and CL, respectively (Fig. 1c–f). The fluorescent tracers Fast Blue (FB), Diamidino Yellow (DY), Fluoro-Ruby (FR) and Fluoro-Emerald (FE) and the tracer BDA (biotinylated dextran amine) were pressure-injected via a Hamilton syringe (200–300 nl per injection, 2 injections per site) or via a glass cannula with a tip diameter of 30 μm (150–300 nanoliters per injection, 2 injections per site). Phaseolus leucoagglutinin (Pha-L; Sigma) was iontophoresed for 20 min at 7.2 μA. The tracers and areas injected in each case were as follows. In case RQ, DY and FE were placed between the 12.5 and 3.2 kHz regions of AL; FB and Pha-L in the 4 kHz region of ML; FR in the 6.3 kHz region of CL. In case JY, FB was placed in the 1.5 kHz region of AL, FR and BDA in the 3 and 8 kHz region of ML and DY in the 3 kHz region of CL. In case DU, FR was placed in the 4 kHz region of AL, DY and BDA in the 4 kHz region of ML and FB in the 4 kHz region of CL. In case C17, FE was placed in the 4 kHz region of AL, FB in the 4 kHz region of ML and FR in the 4 kHz region of CL.

Histology and tissue processing

Monkeys were perfused with 4% paraformaldehyde 10–21 days after recording. Brains were blocked, sunk in increasing sucrose gradients, snap frozen in isopentane and cut at 40 μm on a cryostat. Seven of every ten sections were immediately processed and three sections were saved in freezing medium at 4°C. In a series of ten sections, two or three were immediately mounted onto slides, stored at 4°C and examined for fluorescent labeling. Additional series of sections were processed as follows: one was stained with cresyl violet or thionin, one was stained with parvalbumin (antibody from Sigma, 1:7500 concentration), one was immunohistochemically processed with an antibody to fluoro-ruby and one was immunohistochemically processed with an antibody to fluoro-emerald (cases RQ and C17) or stained for BDA (case JY). In case RQ, one series was immunohistochemically processed for Pha-L. Described cytoarchitectonic borders[43] were estimated from adjacent Nissl sections and sulcal landmarks.

Charting and analysis

Fluorescent labeling in frontal and temporal lobes was examined in coronal sections spaced at 200 μm. Immunohistochemistry for tracers was more sensitive than fluorescence and rendered labeled cells, particularly the anterograde fibers, less susceptible to fading and photo-bleaching. Therefore, anterograde and retrograde labeling with tracers FR and FE were charted from immunohistochemically processed sections; labeling was confirmed by fluorescence in

unprocessed sections. Labeled sections were charted every 400 μm with the Neurolucida plotting system on a Zeiss Axiophot coupled to an LEP stage.

Some temporal sections were also digitally captured with a Spot 2 (Medical Instruments, Germany) video camera. Analysis of the injection sites (Fig. 1) verified that the tracer injections were located on and confined to the dorsal aspect of the superior temporal gyrus and superior temporal plane from which the recordings were made. Tracer injections that spread into the ventral superior temporal gyrus or the superior temporal sulcus were not included in our analysis. Coronal sections were aligned to standard atlas drawings converted to lateral brain schematics of the superior temporal region (Fig. 1). We designated the region recorded and subsequently injected as the lateral belt region based on physiological classification of this non-primary auditory region demonstrated previously[17]. However, some injections may have included portions of the parabelt, whose boundaries are not yet physiologically defined in detail.

The flat map in Fig. 3e is based on the method of Barbas[12]. After mapping anterograde fibers and retrograde cells from coronal sections using the Neurolucida Digital plotting system, a line was drawn through the midpoint of the cortex, approximating layer IV throughout the entire perimeter of the digitized coronal section. This line was then extrapolated to the vertical. Labeled cells and fibers, as well as cytoarchitectonic boundary lines were maintained in appropriate spatial location during this translation. Each coronal section was then aligned along the fundus of the principal sulcus and other sulcal landmarks. Using the drawing program Canvas (ver. 5.0, Deneba), vertical section lines were removed and sulcal boundaries were smoothed, leaving behind retrograde and anterograde plots. Because the anterograde and retrograde labeling were localized to the same regions, lines depicting anterograde labeling were removed for clarity.

Acknowledgments

The authors thank Alexander Kustov, Amy Durham and Aaron Lord for help with electrophysiological mapping, Hisayuki Ojima for help with injections and M. Pappy and J. Coburn for their help with histology. We would also like to thank E. C. Muly, S. O'Scalaidhe and A. Stevens for comments on the manuscript.

References

1. Ungerleider, LG.; Mishkin, M. Analysis of Visual Behavior. Ingle, DJ.; Goodale, MA.; Mansfield, RJW., editors. MIT Press; Cambridge, Massachusetts: 1982. p. 549-586.
2. Wilson FA, O'Scalaidhe SP, Goldman-Rakic PS. Dissociation of object and spatial processing domains in primate prefrontal cortex. Science 1993;260:1955–1958. [PubMed: 8316836]
3. Webster MJ, Bachevalier J, Ungerleider LG. Connections of inferior temporal areas TEO and TE with parietal and frontal cortex in macaque monkeys. Cereb Cortex 1994;4:470–483. [PubMed: 7530521]
4. Buckner RL, Raichle ME, Petersen SE. Dissociation of human prefrontal cortical areas across different speech production tasks and gender groups. J Neurophysiol 1995;74:2163–2173. [PubMed: 8592204]
5. Stromswold K, Caplan D, Alpert N, Rauch S. Localization of syntactic comprehension by positron emission tomography. Brain Lang 1996;52:452–473. [PubMed: 8653390]
6. Gabrieli JDE, Poldrack RA, Desmond JE. The role of left prefrontal cortex in language and memory. Proc Natl Acad Sci USA 1998;95:906–913. [PubMed: 9448258]
7. Stevens AA, Goldman-Rakic PS, Gore JC, Fulbright RK, Wexler BE. Cortical dysfunction in schizophrenia during auditory word and tone working memory demonstrated by functional magnetic resonance imaging. Arch Gen Psychiatry 1998;55:1097–1103. [PubMed: 9862553]
8. Pandya DN, Kuypers HGJM. Cortico-cortical connections in the rhesus monkey. Brain Res 1969;13:13–36. [PubMed: 4185124]
9. Chavis DA, Pandya DN. Further observations on corticofrontal connections in the rhesus monkey. Brain Res 1976;117:369–386. [PubMed: 825194]

10. Petrides M, Pandya DN. Association fiber pathways to the frontal cortex from the superior temporal region in the rhesus monkey. J Comp Neurol 1988;273:52–66. [PubMed: 2463275]
11. Seltzer B, Pandya DN. Frontal lobe connections of the superior temporal sulcus in the rhesus monkey. J Comp Neurol 1989;281:97–113. [PubMed: 2925903]
12. Barbas H. Anatomic organization of basoventral and mediodorsal visual recipient prefrontal regions in the rhesus monkey. J Comp Neurol 1988;276:313–342. [PubMed: 3192766]
13. Hackett TA, Stepniewska I, Kaas JH. Prefrontal connections of the parabelt auditory cortex in macaque monkeys. Brain Res 1999;817:45–58. [PubMed: 9889315]
14. Romanski LM, Bates JF, Goldman-Rakic PS. Auditory belt and parabelt projections to the prefrontal cortex in the rhesus monkey. J Comp Neurol 1999;403:141–157. [PubMed: 9886040]
15. Galaburda AM, Pandya DN. The intrinsic architectonic and connectional organization of the superior temporal region of the rhesus monkey. J Comp Neurol 1983;221:169–184. [PubMed: 6655080]
16. Morel A, Garraghty PE, Kaas JH. Tonotopic organization, architectonic fields, and connections of auditory cortex in macaque monkeys. J Comp Neurol 1993;335:437–459. [PubMed: 7693772]
17. Rauschecker JP, Tian B, Hauser M. Processing of complex sounds in the macaque nonprimary auditory cortex. Science 1995;268:111–114. [PubMed: 7701330]
18. Kosaki H, Hashikawa T, He J, Jones EG. Tonotopic organization of auditory cortical fields delineated by parvalbumin immunoreactivity in macaque monkeys. J Comp Neurol 1997;386:304–316. [PubMed: 9295154]
19. Rauschecker JP, Tian B, Pons T, Mishkin M. Serial and parallel processing in rhesus monkey auditory cortex. J Comp Neurol 1997;382:89–103. [PubMed: 9136813]
20. Hackett TA, Stepniewska I, Kaas JH. Subdivisions of auditory cortex and ipsilateral cortical connections of the parabelt auditory cortex in macaque monkeys. J Comp Neurol 1998;394:475–495. [PubMed: 9590556]
21. Rauschecker JP. Parallel processing in the auditory cortex of primates. Audiol Neurootol 1998;3:86–103. [PubMed: 9575379]
22. Leinonen L, Hyvarinen J, Sovijarvi AR. Functional properties of neurons in the temporo-parietal association cortex of awake monkey. Exp Brain Res 1980;39:203–215. [PubMed: 6772459]
23. Benson DA, Hienz RD, Goldstein MH Jr. Single-unit activity in the auditory cortex of monkeys actively localizing sound sources: spatial tuning and behavioral dependency. Brain Res 1981;219:249–267. [PubMed: 7260632]
24. Hackett TA, Stepniewska I, Kaas JH. Thalamocortical connections of the parabelt auditory cortex in macaque monkeys. J Comp Neurol 1998;400:271–286. [PubMed: 9766404]
25. Rauschecker JP. Cortical processing of complex sounds. Curr Opin Neurobiol 1998;8:516–521. [PubMed: 9751652]
26. Felleman DJ, Van Essen DC. Distributed hierarchical processing in the primate cerebral cortex. Cereb Cortex 1991;1:1–47. [PubMed: 1822724]
27. Goldman-Rakic PS. The prefrontal landscape: implications of functional architecture for understanding human mentation and the central executive. Phil Trans R Soc Lond B Biol Sci 1996;351:1445–1453. [PubMed: 8941956]
28. Fuster, JM. The Prefrontal Cortex. Vol. 2. Raven; New York: 1989.
29. Goldman-Rakic, P. Handbook of Physiology. Section 1: The Nervous System. In: Plum, F., editor. Higher Functions of the Brain. Vol. V. American Physiological Society; Bethesda: 1987. p. 373-418.
30. McCarthy G, et al. Activation of human prefrontal cortex during spatial and nonspatial working memory tasks measured by functional MRI. Cereb Cortex 1996;6:600–611. [PubMed: 8670685]
31. Courtney SM, Ungerleider LG, Keil K, Haxby JV. Object and spatial visual working memory activate separate neural systems in human cortex. Cereb Cortex 1996;6:39–49. [PubMed: 8670637]
32. Goldman PS, Rosvold HE. Localization of function within the dorsolateral prefrontal cortex of the rhesus monkey. Exp Neurol 1970;27:291–304. [PubMed: 4987453]
33. Azuma M, Suzuki H. Properties and distribution of auditory neurons in the dorsolateral prefrontal cortex of the alert monkey. Brain Res 1984;298:343–346. [PubMed: 6722560]
34. Vaadia E, Benson DA, Hienz RD, Goldstein MH Jr. Unit study of monkey frontal cortex: active localization of auditory and of visual stimuli. J Neurophysiol 1986;56:934–952. [PubMed: 3783237]

35. Petrides M. The effect of periarcuate lesions in the monkey on the performance of symmetrically and asymmetrically reinforced visual and auditory go, no-go tasks. J Neurosci 1986;6:2054–2063. [PubMed: 3734876]

36. Bushara K, et al. Evidence for modality-specific frontal and parietal areas for auditory and visual spatial localization in humans. Nat Neurosci 1999;2:759–766. [PubMed: 10412067]

37. Cavada C, Goldman-Rakic PS. Posterior parietal cortex in rhesus monkey: II. Evidence for segregated corticocortical networks linking sensory and limbic areas with the frontal lobe. J Comp Neurol 1989;287:422–445. [PubMed: 2477406]

38. Andersen RA, Snyder LH, Bradley DC, Xing J. Multimodal representation of space in the posterior parietal cortex and its use in planning movements. Annu Rev Neurosci 1997;20:303–330. [PubMed: 9056716]

39. Mazzoni P, Bracewell RM, Barash S, Andersen RA. Spatially tuned auditory responses in area LIP of macaques performing delayed memory saccades to acoustic targets. J Neurophysiol 1996;75:1233–1241. [PubMed: 8867131]

40. Blood AJ, Zatorre RJ, Bermudez P, Evans AC. Emotional responses to pleasant and unpleasant music correlate with activity in paralimbic brain regions. Nat Neurosci 1999;2:382–387. [PubMed: 10204547]

41. Demb JB, et al. Semantic encoding and retrieval in the left inferior prefrontal cortex: a functional MRI study of task difficulty and process specificity. J Neurosci 1995;15:5870–5878. [PubMed: 7666172]

42. Deacon TW. Cortical connections of the inferior arcuate sulcus cortex in the macaque brain. Brain Res 1992;573:8–26. [PubMed: 1374284]

43. Preuss TM, Goldman-Rakic P. Myelo- and cytoarchitecture of the granular frontal cortex and surrounding regions in the strepsirhine primate Galago and the anthropoid primate Macaca. J Comp Neurol 1991;310:429–474. [PubMed: 1939732]

44. Gross CG, Weiskrantz L. Evidence for dissociation of impairment on auditory discrimination and delayed response following lateral frontal lesions in monkeys. Exp Neurol 1962;5:453–476. [PubMed: 13902195]

45. Lawicka W, Mishkin M, Rosvold HW. Dissociation of impairment on auditory tasks following orbital and dorsolateral frontal lesions in monkeys. Proc Congr Polish Physiol Soc 1966;10:178.

46. Iversen SD, Mishkin M. Perseverative interference in monkeys following selective lesions of the inferior prefrontal convexity. Exp Brain Res 1970;11:376–386. [PubMed: 4993199]

47. Tanila H, Carlson S, Linnankoski I, Kahila H. Regional distribution of functions in dorsolateral prefrontal cortex of the monkey. Behav Brain Res 1993;53:3–71.

48. Bodner M, Kroger J, Fuster JM. Auditory memory cells in dorsolateral prefrontal cortex. Neuroreport 1996;7:1905–1908. [PubMed: 8905689]

49. Benevento LA, Fallon J, Davis BJ, Rezak M. Auditory–visual interaction in single cells in the cortex of the superior temporal sulcus and the orbital frontal cortex of the macaque monkey. Exp Neurol 1977;57:849–872. [PubMed: 411682]

50. O'Scalaidhe SP, Wilson FA, Goldman-Rakic PS. Areal segregation of face-processing neurons in prefrontal cortex. Science 1997;278:1135–1138. [PubMed: 9353197]

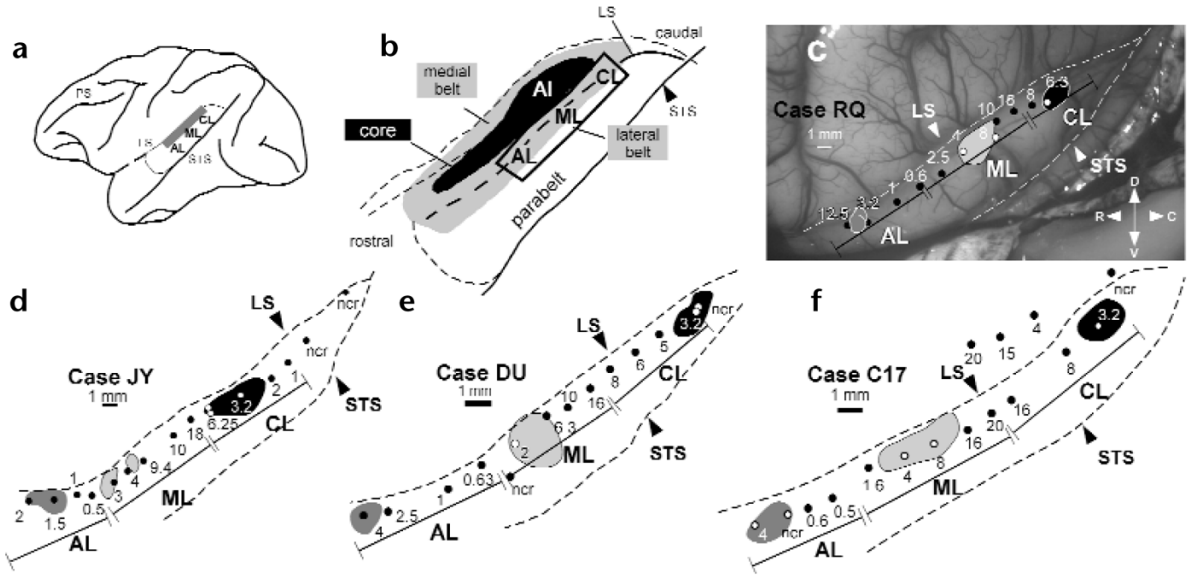

Fig. 1.

Tonotopic maps of the lateral belt region recorded in four monkeys. (**a**) Lateral belt region (shaded in gray) overlies the superior temporal plane and dorsal aspect of the superior temporal gyrus. (**b**) The same region, enlarged to show the locations of the medial and lateral belt (shaded in gray), primary auditory cortex (AI, black) and the parabelt cortex on the superior temporal gyrus. The portion of the lateral belt recorded from is outlined. (**c–f**) Physiological maps of the lateral belt recordings from each of the four monkeys in a schematic of the superior temporal region. (**c**) Photomicrograph taken during the electrophysiological recordings of the lateral belt in case RQ. (**d–f**) Mappings from the other three cases. The best center frequency for each electrode penetration (black or white dots) is labeled in kHz. Injections of different anterograde and retrograde tracers (shaded regions) for each case are shown with respect to these recordings (for details of tracers in each case see Methods). The boundaries of AL, ML and CL are delineated by a bounded line and are derived from the frequency reversal points. Abbreviations: ncr, no clear response for this electrode penetration, LS, lateral sulcus; PS, principal sulcus; STS, superior temporal sulcus; D, dorsal; V, ventral; R, rostral; C, caudal.

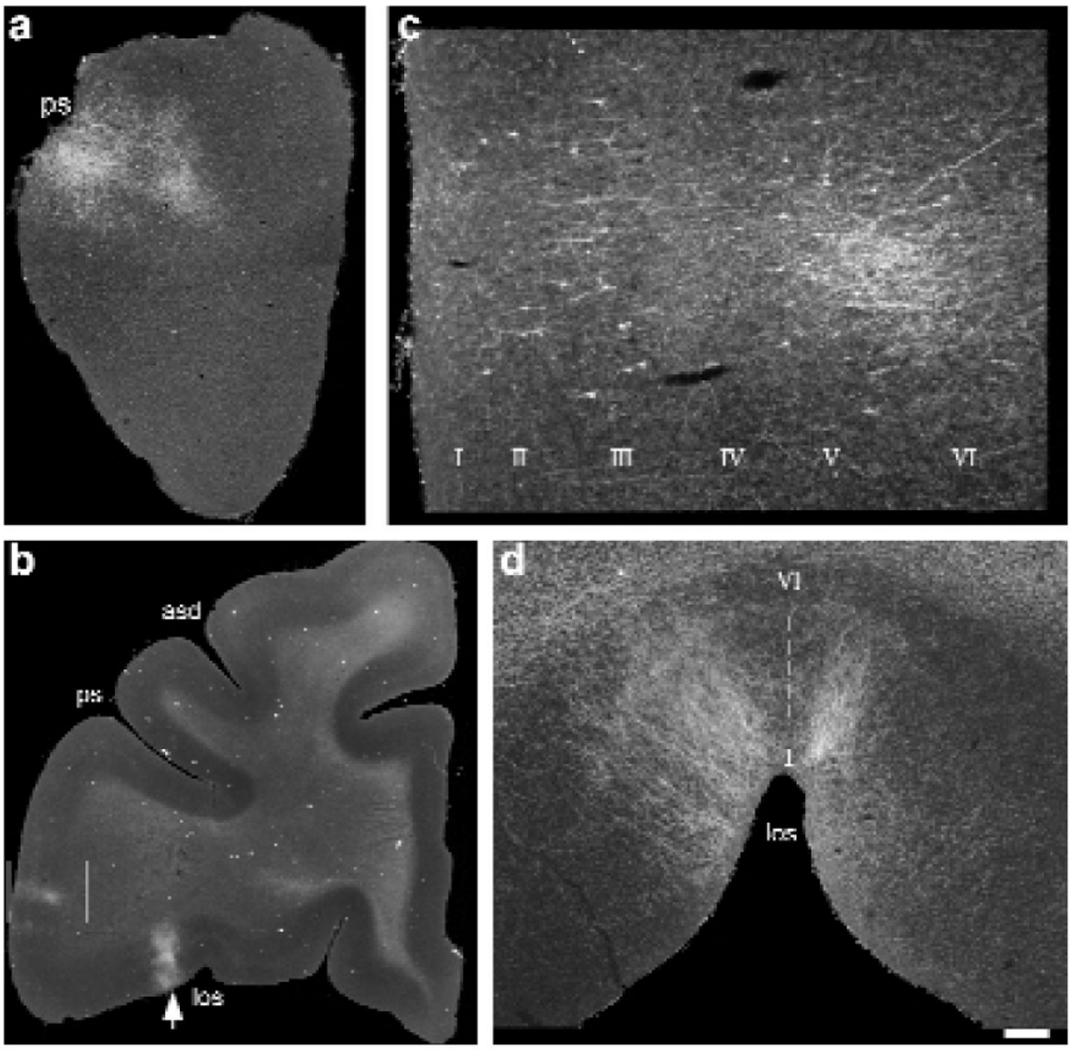

Fig. 2.

Photomicrographs of anterograde and retrograde labeling in the rostral and ventral regions of the prefrontal cortex after injections of Fluoro-ruby (**a**, **d**; case DU) or Fluoro-Emerald (**b**, **c**; case RQ) into area AL. (**a**) Low-power photomicrograph of anterogradely labeled fibers in a coronal section through the frontal pole region, just anterior to the beginning of the principal sulcus. (**b**) Low-power photomicrograph from a coronal section with labeling in the lateral inferior convexity (boxed region) and the lateral orbital cortex (arrow). (**c**) The boxed region at higher power. Cells in layers III and V were retrogradely labeled, whereas anterogradely labeled fibers were seen in layers II, III, V and VI. (**d**) Photomicrograph of the same lateral orbital region (**b**; arrow) from a different case (DU), detailing the lateral orbital projections at higher magnification in a coronal section in which they were densest. Labeled axons made columnar terminations spanning all layers (I–VI) at the juncture of the lateral orbital sulcus. Scale bar (**a**) 600 μm; (**b**) 2250 μm; (**c**)250 μm; (**d**) 425 μm. Abbreviations: asd, dorsal arcuate sulcus; los, lateral orbital sulcus; ps, principal sulcus.

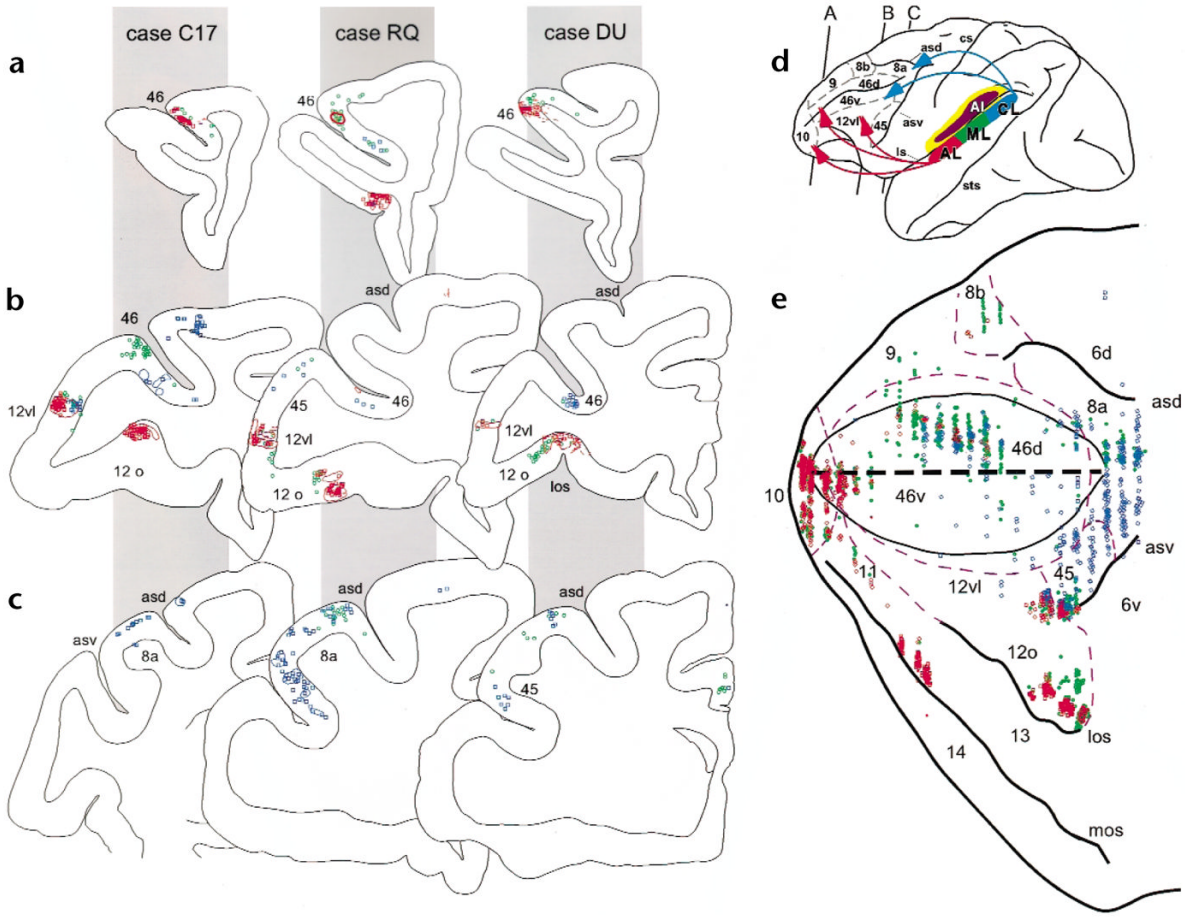

Fig. 3.

Anterograde and retrograde labeling in the prefrontal cortex. In three monkeys (cases C17, RQ and DU indicated by gray panels) coronal sections from anterior (**a**), middle (**b**) and posterior (**c**) levels of the prefrontal cortex are shown with color coded retrograde cells (dots and squares) and anterograde fibers (outlined shapes). The cytoarchitectonic region is shown next to the labeling in each coronal section. Across all cases, projections from injections into AL (red) were found in the frontal pole (not shown), the rostral principal sulcus (level **a**) and in the lateral inferior convexity and lateral orbital cortex (level **b**). In contrast, projections from CL (blue) can be seen in more caudal principal sulcus regions in (**b**) as well as in the periarcuate cortex shown in (**c**)and also in the lateral inferior convexity in (**b**). Projections from area ML, shown in green, overlapped with projections from AL and CL. (**d**) Lateral brain schematic showing color coding of the lateral belt injections and the cytoarchitectonic organization of the prefrontal cortex as well as the rostrocaudal levels of the coronal sections from (**a–c**). Projections are summarized with arrows. (**e**) Flattened map of dorsolateral and ventral prefrontal cortex showing the projections from case RQ shows that AL projections (red) target 10, rostral 46 and ventral prefrontal regions (areas 12vl, l2o and 45) whereas CL (blue) targets the caudal principal sulcus and periarcuate regions (caudal 46 and 8a) and the lateral inferior convexity (areas 12vl and 45). The dashed purple lines indicate described cytoarchitectonic borders[43] and edges of major sulci are shown in black. The center black dashed line represents the principal sulcus.